JOURNAL OF APPLIED ELECTROCHEMISTRY 4 (1974) 211–218

Electrocatalytic activation of tungsten and tungstic oxide doped with platinum by means of ion implantation

M. GRENNESS, M. W. THOMPSON

School of Mathematical and Physical Sciences

and R. W. CAHN

School of Applied Sciences, University of Sussex

Received March 20 1974

Minute quantities of platinum have been introduced into substrates of tungsten and tungstic oxide by means of ion implantation. In this way significant effects on the rate of the cathodic hydrogen evolution reaction have been demonstrated in which the electrocatalytic activity of the surface approaches that of platinum itself.

1. Introduction

The efficiency of electrochemical processes such as the electrolysis of water or the generation of power from fuel cells is limited by the departure of the electrodes from reversible behaviour. The departure is recognized as a deviation from the reversible electrode potential which is referred to as the overpotential, and it leads to ohmic losses in the cell in addition to those already incurred by the resistance of the electrolyte. For any fixed current through the cell, however, the overpotential varies with the chosen electrode material according to its properties as an electrocatalyst and can be greatly reduced by using various metals, mostly from the platinum group. Platinum, so far, has been shown to be the best material for this purpose. Because of its cost and limited availability there is every incentive to create conditions where the smallest possible quantities would be required. For this reason experiments with ion implantation are being carried out to determine whether minute quantitities of platinum injected into surface layers of a base-metal, acting as a catalyst support, could effectively substitute for the much heavier surface applications often used. This paper reports on the first phase of this investigation.

The technique of ion implantation has been developed during the past decade as a means of introducing foreign atoms into the surface layers of a solid. So far, ion implantation has mostly been applied in the production of semiconductor devices [1] but other applications are being developed [2–4]. Ion implantation is carried out *in vacuo* where the implant species, provided as free ions, is accelerated by means of an ion accelerator of the type used in mass spectrometers [1,5] and the substrate which is to be doped is placed as the target in the ion beam. When moving ions impinge on the target, physical processes take place which damage and alter the properties in a thin layer of the target. Most of the energy is transferred to the target through primary and secondary collisions and collision cascades [5,6] in which a large number of atoms are sputtered away (including scattering of a few of the incident particles); the remaining ions and recoiled target atoms lodge in the target, generating crystal defects. In the first stages, when an increasing number of particles lodge in the substrate, a concentration distribution in depth develops gradually; the distribution depends principally on the mass ratio M_1/M_2 of the ion and target atoms, respectively, the atomic number of the ion and the kinetic energy [6-8]. (It depends also on the natute of the target material, e.g. amorphous or crystalline: in crystals, channelling occurs [5,6]). With a large M_1/M_2 ratio, the profile is approximately a Gaussian distribution with virtually zero concentration at the surface; the depth of the peak concentration can be estimated using Nielsen's formula [7]. Conversely with a small M_1/M_2 ratio the peak concentration is at the surface itself, tapering off with depth. With an M_1/M_2 ratio about unity the distribution takes the form of a peak skewed towards the surface with a substantial concentration at the surface.

When the dose exceeds 10^{15} ions cm^{-2} the situation is considerably complicated and the concentration profile is distorted. Firstly, the M_1/M_2 ratio progressively changes with increasing dose since previously implanted atoms effectively become target atoms (unless $M_1/M_2 \sim 1$ initially). Secondly. the surface layers are eroded away by the sputtering which has the effect of moving the peak towards the final surface. Thirdly, radiation-enhanced diffusion becomes significant, because collision cascades tend to move the implanted atoms, and mobile point defects created by the collision cascades accelerate normal diffusion. This reduces the concentration gradient in the system and flattens the peak of the concentration distribution.

Apart from the effects of diffusion, the sputtering ratio, i.e. the number of atoms sputtered per incident ion, has a controlling effect on the concentration of the implant. The sputtering ratio, which depends on the M_1/M_2 ratio, the kinetic energy and the binding energy of the target atoms [5,6,9,10] is usually larger than unity and is often of the order of 10. Assuming that the implant atoms sputter at the same rate as the target atoms and neglecting the effects of diffusion, the maximum possible peak concentration would be the inverse of the sputtering ratio.

This article describes the electrocatalytic effects produced by ion implantation of platinum into substrates of tungsten and tungstic oxide. These substrates were chosen partly because tungsten has a fairly high atomic mass and thus the M_1/M_2 ratio is kept down (which favours higher surface concentrations of platinum), and partly because of the interest in examining the effect of implanted electrocatalyst on the behaviour of semiconducting tungstic oxide, which can under certain circumstances be electrochemically converted into a metallic conductor [14–17]. In these cases, with a kinetic energy typically of 200 keV, the scattering by tungsten atoms dominates that by oxygen and the effective value of M_1/M_2 is close to unity in both cases. At low doses, e.g. 10^{13} ions cm^{-2}, the surface concentration is estimated to be 1/10 relative to the peak concentration. There are no data available with regard to the sputtering rates but if the implanted atoms sputter less rapidly than the target atoms and there is no diffusion over a distance comparable to the range of penetration, then the surface concentration could reach 100% for a high dose (e.g. 10^{16} ions cm^{-2}). In the electrochemical experiments the effects were studied employing the cathodic hydrogen evolution reaction in 1 M sulphuric acid, by means of the potentiostatic method.

2. Experimental

The working electrodes (also referred to as 'the samples') were made from 3 mm diameter tungsten rods with a purity of 99·95%, the major impurities being molybdenum (280 p.p.m.), iron (150 p.p.m.), a little Ni (30 p.p.m.) and Cr (20 p.p.m.). (Traces of other metals present do not include noble metals.) One end of a rod was fused into a glass seal which was then fused to the end of a 2 ml syringe plunger. The tip of the tungsten rod and seal was ground and polished optically flat.

A chosen electrode was placed in a syringe barrel, which had been fused as a side arm on to a conventional three-compartment cell. A saturated calomel electrode (SCE) was used as reference and the counter electrode was made of vitreous carbon. Various gases could be introduced through a sintered glass disc in the bottom of the working electrode compartment.

All solutions were prepared from A.R. grade chemicals and triply distilled water. All glassware was cleaned in alcoholic potassium hydroxide followed by a H_2SO_4/HNO_3 mixture and thoroughly rinsed in triply distilled water prior to use. Immediately prior to an electrochemical experiment, the working electrode was dipped into chromic acid and rinsed with triply distilled water. Potentials were controlled in the usual way by a potentiostat coupled to a waveform generator. Slow-sweep, 'steady-state' current-voltage curves and cyclic voltammograms (typically at 0·3 mV s^{-1} to 3 mV s^{-1}), were recorded directly on an X-Y recorder.

Half the samples were anodized prior to implantation. This was carried out in 0·4M KNO_3+0·04M HNO_3 solution following a procedure used by McCargo *et al.* [11]. This procedure employed a constant current of 2 mA cm^{-2} until the required voltage was reached and then at constant voltage until the current was well below 100 μA cm^{-2}. The thickness of the oxide film varies linearly with the applied voltage [11] and is of the order of 110 nm at 72 V. The expected current decay was not achieved initially, but did appear after a few repeated attempts; between attempts the oxide film was stripped in 1% NaOH solution. Tungstic oxide films, WO_3, produced in this way are known to be non-crystalline or at least the crystals are extremely small (~3 nm) [11].

Ion-implantation was carried out at A.E.R.E., Harwell with the 400 kV Cockcroft–Walton accelerator. The platinum was vapourized and ionized in a sputtering ion source [6]. The Pt^+ ions were accelerated to an energy of 200 keV, ions of different mass number, energy and charge being separated by means of an analysing magnet. In order to minimize contamination of the electrode samples, the target chamber was evacuated using turbo-molecular pumps and ion pumps with cold traps at the entrance. Doses of 2×10^{15}–2×10^{16} ions cm^{-2} were implanted.

Nielsen's formula [7] was used to make a rough estimate of the range of penetration in the oxide layer, which was assumed to be amorphous WO_3. Using a weighted average atomic mass, the kinetic energy of the platinum ions of 200 keV, and taking the specific density of the tungstic oxide as 7·2 g cm^{-3}, the range was found to be in the order of 35 nm.

3. Results

Fig. 1 shows some typical current-voltage measurements for the hydrogen evolution reaction with nitrogen passing through the solution. The logarithm of the current is plotted against the electrode potential (versus SCE) and the measurements were obtained by applying slow potential scans to the potentiostat. Curve I is for untreated tungsten polarized cathodically. The current is slightly increased on the reverse sweep (not shown). Curve IIA is obtained for anodized tungsten (thickness of oxide film = 90 nm). The surface is considerably activated during this cathodic sweep and the performance approaches that of the untreated tungsten on the reverse sweep, curve IIB, (sweep rate = 3 mV s^{-1}). This hysteresis effect was duplicated on the second polarization sweep. Curve III shows the perform-

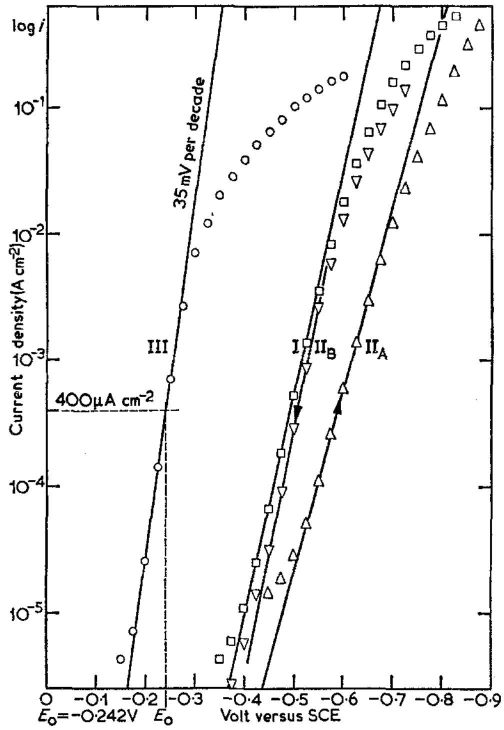

Fig. 1. Cathodic H_2 evolution. Solution: nitrogen-saturated M H_2SO_4. E_0 is the reversible hydrogen electrode potential (−0·242 V versus SCE).

I: Untreated tungsten.

II: Tungsten anodized at 60 V (thickness of film 90 nm).

III: Tungsten anodized at 60 V, Pt-implanted. Dose 2×10^{15} ions cm^{-2}. Energy 200 keV.

ance of an anodized and implanted sample. The dose was 2×10^{15} ion cm^{-2} corresponding to $0{\cdot}65\ \mu g\ cm^{-2}$ (or the equivalent of $1\frac{1}{2}$ monolayers of Pt). At less negative potentials there is a linear relationship between log i and potential and the slope is 35 mV per decade of current (Tafel slope). The performance in this region is nearly that of bright platinum, which exhibits a Tafel slope of 29·6 mV per decade under similar conditions. At the reversible hydrogen electrode potential, i.e. −0·242 V versus SCE, a current of 400 μA is observed.

This current is a measure of the exchange current and if the solution were saturated in hydrogen instead of nitrogen, the reverse reaction, i.e. the anodic ionization of hydrogen, would proceed at the same rate. As a result there would be equilibrium and the net current would be zero. (When the performance in this article is referred to as 'high' it is implied that the Tafel slope is in the region of 30 mV per decade of current and that the current at the reversible hydrogen electrode potential is larger than $\sim 100\ \mu A\ cm^{-2}$).

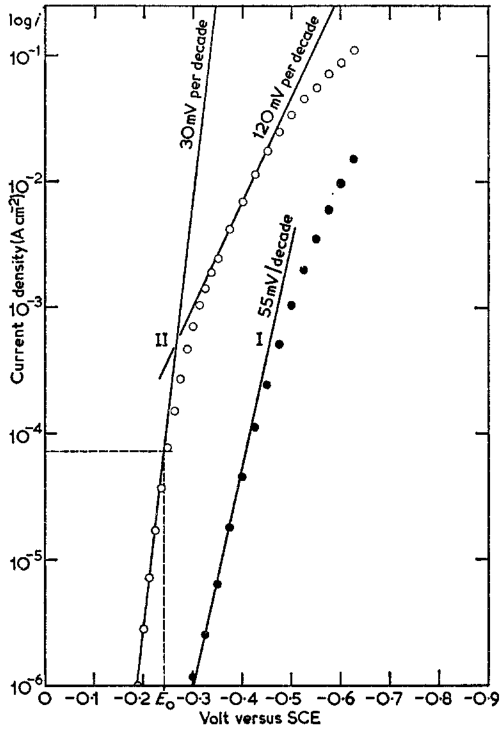

Fig. 2. Electrode: tungsten anodized at 72 V (110 nm) Pt-implanted. Dose 2×10^{15} ions cm^{-2}.
I: Initial cathodic sweep.
II: Sweep number 4.

The high performance, as shown in Fig. 1, curve III, is not normally exhibited initially on a freshly implanted sample, but is obtained after various 'conditioning' treatments. In the case of electrodes which have been anodized prior to implantation the high performance developed after a few repeated cathodic polarization sweeps (see Fig. 2) or after the electrode has been held at negative potentials in the region −0·5 to −0·7 V for several minutes. Also, the electrode can be activated, after an initial cathodic polarization test, by exposing it to air for a few days. Curve III of Fig. 1 was obtained with an electrode treated in this way.

In the case of samples which were implanted with platinum without anodization, the initial performance was usually lower than for those which were anodized and at larger negative potentials the performance was even lower than for untreated tungsten. (Compare curve I, Fig. 3, with curve I on Figs. 1 and 2). Repeated cathodic polarization sweeps did not increase the performance significantly whereas *anodic* treatments usually did. In these treatments the electrode potential was ramped to +3 V. An example of this effect is described below where the hydrogen evolution reaction was studied before and after three anodic sweeps. In the first anodic sweep, the current rose sharply near 2 V and went through a maximum of 100 mA cm^{-2} at +2·35 V. This was thought to be due to oxygen evolution but as the current went through a maximum it is possible that platinum was dissolved at the same time. Peaks of this magnitude were absent in the second and third sweeps. Nevertheless, the electrode exhibited a considerable improvement in performance of the hydrogen evolution reaction in the following cathodic polarization sweep as shown in Fig 3, curve II. The platinum dose in this case, however, was ten times larger than usual, i.e. 2×10^{16} ions cm^{-2}. However, electrodes suffer following repeated sweeps to *high anodic* potentials (3 V): the performance appears to decrease progressively. Another electrode, which was not anodized before implanation, exhibited the high performance after the initial cathodic polarization test and after being left in distilled water for 2 days and in dry air for 6 h.

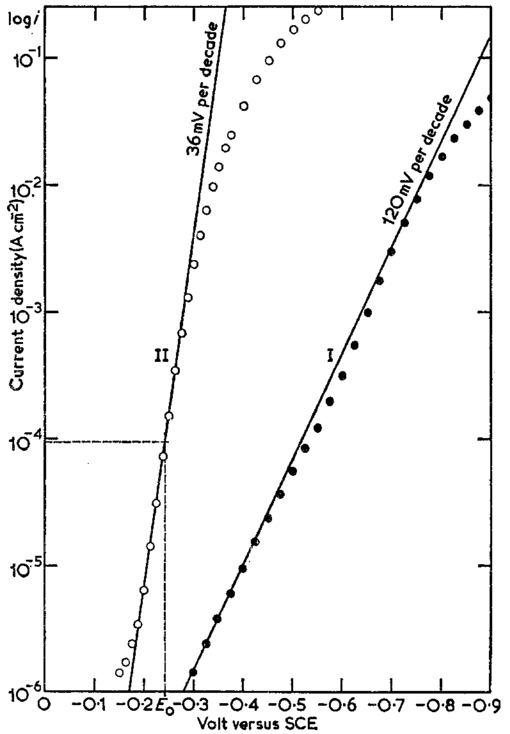

Fig. 3. Electrode: tungsten (not anodized), Pt-implanted. Dose 2×10^{16} ions cm^{-2}.
I: Initial cathodic sweep.
II: Cathodic sweep after anodic treatment, i.e. three anodic sweeps to +3 V.

In another experiment with an electrode anodized before implantation and implanted at a dose of 2×10^{15} ions cm^{-2}, the oxide film was dissolved in KOH solution immediately before the polarization experiment. Some platinum must have remained on the surface since the high performance was apparent without further activation.

4. Discussion

4.1 *Mechanism of activation: anodized electrodes*

It is not clear at present why the doped electrodes are required to be activated as described and what the mechanism is. At small doses, e.g. 10^{13} ions cm^{-2}, the platinum at the surface is likely to be very finely dispersed, assuming that there is little solid-state diffusion and agglomeration. On such a surface, isolated islands of platinum, perhaps consisting of only a few atoms or even single atoms, may occur which adsorb only a single H atom at a time. Under these conditions surface diffusion of hydrogen and the charge transfer step, i.e.

$$H^+ + e^- \rightarrow H_{ads}$$

might be the slow step in the cathodic reaction $2H^+ + 2e^- \longrightarrow H_2$, as on pure untreated tungsten, and there is no net enhancement of the activity.

However, the doses of platinum actually implanted were orders of magnitudes larger, e.g. 2×10^{15} and 2×10^{16} ions cm^{-2}. Thus, if there is any tendency for platinum atoms to segregate into separate phases in either tungstic oxide or metallic tungsten, these high doses would favour it. Available evidence on solid solubilities of noble metals in amorphous oxides is confined mainly to silver and gold in glasses [12] and in these there is a well-known tendency for the metal atoms to segregate at low temperature. Similarly it is known that the solid solubility of platinum in metallic tungsten is small at room temperature, i.e. ~4–6 at % [13]. In view of this and the likelihood of radiation-enhanced diffusion, one would expect there to be quite large agglomerates of platinum embedded in the surface and hence the electrode should be active initially, which is in conflict with the experimental evidence.

The activation, however, could be facilitated by the presence of the tungstic oxide, where mechanisms similar to those proposed by Hobbs and Tseung [14–16] may occur, which involve the so-called 'bronze route'. They used porous hydrophobic fuel cell type electrodes and studied the anodic oxidation of hydrogen on catalysts prepared from WO_3 powder, doped with platinum by means of freeze-drying techniques followed by heat-treatment. In the suggested mechanism, hydrogen atoms, adsorbed on platinum, readily react with tungstic oxide in the presence of water [17] to form hydrogen-tungsten bronzes. Since tungsten-bronzes are known to be metallic conductors, the hydrogen in the bronze which is also in contact with the solution is readily ionized. The proposed *anodic* mechanism is

$$\frac{1}{x}\,WO_3+(H\text{—}Pt) \rightleftarrows \frac{1}{x}\,H_xWO_3+Pt \qquad (1)$$

$$\frac{1}{x}\,H_xWO_3 \rightleftarrows \frac{1}{x}\,WO_3+e^-+H^+ \qquad (2)$$

$$(0<x<1)$$

where the charge transfer reaction is thought to be a slower step than those involving adsorption and migration to the oxide. By means of this 'bronze route', the overall hydrogen ionization reaction was thought to take place over a larger fraction of surface area than that actually occupied by platinum.

Tungsten bronzes, doped with platinum, in particular sodium tungsten bronzes, have received considerable attention in recent years as catalysts for the hydrogen and oxygen ionization reactions. Originally, the catalytic properties were credited to the bronzes themselves (Sepa, Damjanović and Bockris [18, 19]), but Bockris and McHardy [20] showed later that the bronzes only possess these properties if traces of platinum are present. Randin *et al.* [21,22] also worked with tungsten bronzes and discussed bronze route mechanisms similar to those of Hobbs and Tseung [19–16]. There might, in fact, be several distinct mechanisms involving a 'bronze route'. perhaps depending on whether the hydrogen is being ionized or discharged. The existence of two distinct Tafel slopes, as in Figs. 2 and 3, indicates that even at the cathode alone two different rate-determining steps may apply, according to overpotential.

As an alternative to the 'bronze route' mechanism, it is possible that the activation of anodized and implanted samples is due simply to a cathodic reduction of the oxide layer, in which platinum possibly is uncovered or diffuses to the surface in sufficient concentration, so that a 'conventional' H_2 evolution reaction can take place as on bright platinum. This view is supported by the fact that the surface changes colour after each cathodic activation sweep and continues to change after each polarization sweep until the surface is colourless like tungsten itself. The alternative view is also supported by the experiment where the oxide film was dissolved in strong KOH solution and the electrode became active.

4.2. *Mechanism of activation: non-anodized electrodes*

In the case of tungsten substrates which were not anodized before the implantation and required an anodic treatment to activate the surface (Fig. 3), a thin oxide film is formed; oxygen evolution also occurs and, depending on the anodic potential limit, platinum may also dissolve. Then during the following cathodic sweep the oxide is dissolved, uncovering more platinum. It is possible however, that the implanted platinum moves during the anodizing process. It could either diffuse to the surface or, perhaps more likely (depending on the voltage) retreat before the advancing oxide front during the anodization. This kind of behaviour has been demonstrated for various metals implanted into aluminium before anodization [21–23].

When an electrode which has been anodized before implantation was given a heavy dose of 2×10^{16} ions cm^{-2}, it was noticed that the elec-

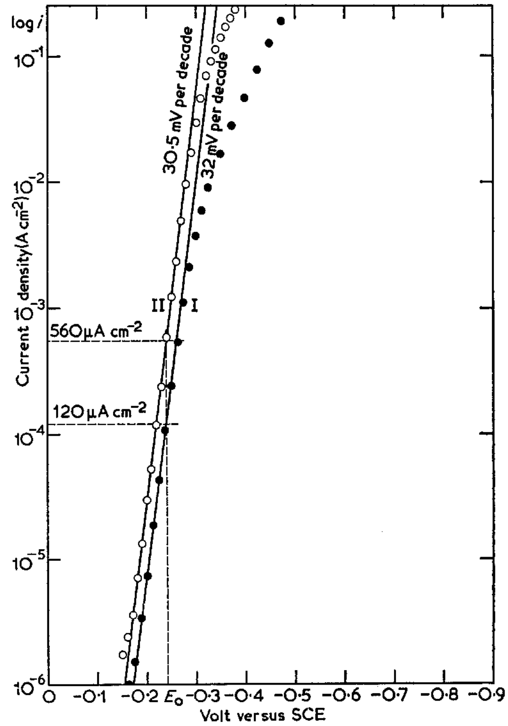

Fig. 4. Electrode: tungsten anodized at 72 V, Pt-implanted. Dose 2×10^{16} ion cm^{-2}.

I: After activation. Few cathodic sweeps.

II: After cyclic voltammetry experiment recorded on Fig. 5.

trode surface appeared metallically bright after the implantation whereas it had a pink colour after the preceding anodization. Although there are no data on the relative sputtering ratios of the component atoms from a W-O-Pt system, it is known from studies of pure tungsten oxides (R. Kelly, private communication) that oxygen sputters more readily than tungsten and at doses of this magnitude, corresponding to the equivalent of fifteen monolayers of Pt, it is expected that very little oxygen would be present.

The electrode was activated as described before, by means of a few cathodic sweeps, although its initial performance was already quite high. Fig. 4, curve I, shows the activated performance. The electrode was then subjected to a series of potential sweeps (cyclic voltammetry) with a cathodic potential limit fixed at −0·24 V and the anodic limit gradually increased from +0·3 V to +1·5 V. The sweep rate was 100 mV s^{-1} and Fig. 5 shows the initial, two intermediate, and the final voltammograms. The initial voltammogram (a) is rather featureless but as the positive voltage is increased (b and c) various peaks develop at the cathodic (right) end. The final voltammogram (heavy line) bears a striking resemblance to that obtained on bright platinum under similar conditions which is shown (dashed line) for comparison. Over large regions the two voltammograms coincide perfectly. The peaks labelled 1 and 2 are the usual adsorption peaks for hydrogen and similarly 3 and 4 the desorption peaks. (These four peaks, however, do not need to develop, being present initially, if this experiment is done on bright platinum.) On the final voltammogram this region is somewhat obscured, although the four peaks are clearly visible; this is believed to be due to impurities from solution adsorbing and desorbing but the formation and oxidation of hydrogen tungsten bronzes would possibly also appear in this region. The large anodic

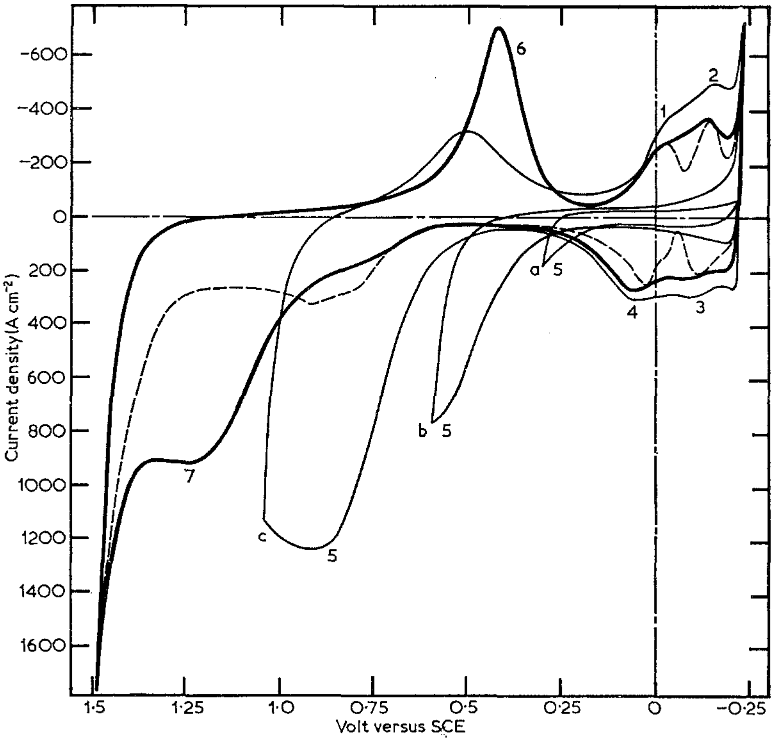

Fig. 5. Cyclic voltammetry experiment on Pt-implanted tungsten. Solution: nitrogen-saturated M H_2SO_4. Electrode: tungsten, anodized at 72 V, Pt-implanted: dose 2×10^{16} ions cm^{-2}.
Initial voltammogram (a): positive limit 0·3 V.
Two intermediate voltammograms: (b, c), positive limits 0·6 V and 1·1 V versus SCE.
Final voltammograms: heavy line, positive limit: 1·5 V versus SCE.
Reference voltammogram on Pt: dashed line.
Ramp rate (all): 100 mV s^{-1}.

current on the initial and intermediate voltammograms (labelled 5) is due to oxidation of tungsten. As the anodic potential limit is increased, the large current reappears after each cycle gradually more to the left, i.e. at larger anodic potentials. This is due to the thickening of the oxide film on the tungsten. At potential limits more positive than 0·9 V the peak 6 begins to appear and is fully developed at limits in the region of 1·3 V. The platinum is oxidized in the anodic sweep at potentials more positive than 0·8 V (dashed line), and peak 6 is due to the surface reduction of oxidized implanted platinum: the development of this peak is identical to that on bright platinum. Peak 7 on the final voltammogram is not at present understood.

The heights of the four hydrogen peaks and the oxide reduction, peak 6, indicate that a large proportion of the tungsten is covered by platinum or became covered after the cyclo-voltammetric experiment. This is perhaps not surprising, taking into account the large dose of platinum implanted. Another cathodic polarization sweep was carried out following this experiment and is recorded on Fig. 4, curve II. Note that the linear relationship with the 30 mV per decade Tafel slope is retained for at least one more decade of current as compared to any of the previous discussed performances. This suggests that repeated cycling does not cause electrode deterioration, but on the contrary causes improvement, if the anodic potential is not allowed to rise too high.

5. Conclusion

In view of the occasionally contradictory evidence the conclusions regarding mechanisms can only be speculative at this stage. The study is continuing in order to establish: (1) the mechanism of formation and role of the tungstic oxide layer (2) the distribution and movements of the platinum, (3) the effect of varying the dose and conditions of implantation and (4) the kinetics of the hydrogen evolution reaction.

Acknowledgements

The authors are indebted to the Science Research Council for financial support of this investigation, and to the Nuclear Physics Division of A.E.R.E., Harwell for carrying out the ion implantation.

References

[1] J. W. Mayer, L. Eriksson and J. A. Davies, 'Ion Implantation in Semiconductors', Academic Press, New York, London (1970).
[2] J. E. Antill *et al.*, AERE-R7471, Harwell (1973).
[3] N. W. Suffield, AERE-R7395, Harwell (1973).
[4] N. E. W. Hartley, G. Dearnaley and J. F. Turner, AERE-R7441, Harwell (1973) and *J. Mater. Sci.*, **8** (1973) 900–4.
[4a] N. E. W. Hartley, G. Dearnaley, J. F. Turner and J. Saunder, AERE-R 7580 Harwell (1973)
[5] M. W. Thompson, 'Defects and Radiation Damage in Metals', Cambridge University Press (1969).
[6] R. S. Nelson, 'The Observation of Atomic Collisions in Crystalline Solids', North-Holland Publishing Co., Amsterdam (1968).
[7] K. O. Nielsen, 'The Range of Atomic Particles with Energies above 50 keV', In *Electromagnetically Enriched Isotopes and Mass Spectrometry*, Ed. M. L. Smith, Butterworth, London (1956).
[8] J. Lindhart, M. Scharff and H. E. Schiott, 'Notes on Atomic Collisions II, III, *Mat. Fys. Jedd. Dan.* Vid. Selsk., **33** (1963) nr 14; *ibid.*, **33** (1963) nr 10.
[9] O. Almén and G. Bruce, *Nuclear Instruments and Methods* **11** (1961) 257–78; *ibid.*, **11** (1961) 279–89.
[10] G. Carter, J. N. Baruah and W. A. Grant, *Radiation Effects*, **16** (1972) 101–5.
[11] M. McCargo and J. A. Davies and F. Brown, *Canadian Journal of Physics*, **41** (1963) 1231.
[12] G. P. Smith, private communication; and *IEEE Spectrum* 3 (1966) 39.
[13] M. Hansen, 'Constitution of Binary Alloys', McGraw-Hill Book Co., (1958).
[14] B. S. Hobbs and A. C. C. Tseung, *Nature*, **222** (1969) 556–8.
[15] B. S. Hobbs and A. C. C. Tseung, *J. Electrochem. Soc.*, **119** (1972) 580–3.
[16] B. S. Hobbs and A. C. C. Tseung, *ibid.*, **120** (1973) 766–9.
[17] J. E. Benson, H. W. Kohn and M. Boudart, *Journal of Catalysis*, **5** (1966) 307–13.
[18] D. B. Sepa, A. Damjanović and J. O. M. Bockris, *Electrochim. Acta.*, **12** (1967) 746.
[19] A. Damjanović, D. B. Sep and J. O'M. Bockris, *J. Res. Inst. Catalysis*, **16** (1968) 1.
[20] J. McHardy and J. O'M Bockris, *J. Electrochem. Soc.*, **120** (1973) 53–66.
[21] J. P. Randin, A. K. Vijh and A. B. Chughtai, *ibid.*, **120** (1973) 1174–1184.
[22] J. R. Pandin, *ibid.*, **120** (1973) 378–81.
[23] W. D. Macintosh, F. Brown and H. H. Plattner, Progress report. Chemistry and Materials Division, Chalk River Nuclear Laboratories, October–December 1972 and January–March 1973, and Conference paper, Albuquerque, New Mexico 1973.
[24] F. Brown and W. D. Macintosh, *J. Electrochem. Soc.*, **120** (1973) 1096–1102.
[25] G. Dearnaley, 'The Use of Ion Beams in Corrosion Science', Conference paper, Albuquerque, New Mexico, 1973.
[26] R. Kelly, Private Communication.